Smooth exterior complex-scaling, full-angular-momentum, and three-dimensional finite-element method applied to doubly excited states of helium

Nils Elander,[1] Sergey Levin,[1,2,3] and Evgeny Yarevsky[2,4]
[1]*Department of Physics, Stockholm University, Alba Nova University Center, SE-106 91 Stockholm, Sweden*
[2]*Institute for Physics, St. Petersburg University, Uljanovskaya 1, St. Petersburg 198904, Russia*
[3]*The Institute for Theoretical Atomic and Molecular Physics at Harvard University and Smithsonian Astrophysical Observatory, 60 Garden Street, MS 14 Cambridge, Massachusetts 02138, USA*
[4]*International Solvay Institutes for Physics and Chemistry, Case Postale 231, Campus Plaine ULB Boulevard du Triomphe, Brussels 1050, Belgium*

(Received 19 June 2002; revised manuscript received 25 March 2003; published 27 June 2003)

A technique based on the total-angular-momentum representation the smooth exterior complex-scaling procedure, and the three-dimensional finite-element method, is applied to calculations of *S*, *P*, and *D* resonant, so-called doubly excited, states of the helium atom. The resonances are calculated with an accuracy better than 10^{-5} a.u. The applicability of an extrapolation procedure to complex energies is analyzed.

DOI: 10.1103/PhysRevA.67.062508 PACS number(s): 31.15.−p, 21.45.+v, 02.70.−c, 32.80.Dz

I. INTRODUCTION

The fully three-dimensional Schrödinger problem finds applications in many different areas of physics and chemistry. For example, in the theoretical description of some halo nuclei and their fragmentation in nuclear physics it is often assumed that the system can be approximated with heavy core nuclei that are tightly bound and a pair of loosely bound neutrons or protons [1]. Optical transitions in exotic atomic systems, such as the antiprotonic helium, have recently been studied to high accuracy [2]. Since the interparticle interactions in many atomic systems are to high accuracy of pure Coulombic nature, they thus offer themselves as test benches for accurate computational models.

We have for the past few years tried to develop and apply a numerical method that allows the determination of energies and fragmentation (for example, autoionization or predissociation) widths for an arbitrary three-dimensional system describable within the Schrödinger framework. Starting with the antiprotonic helium system, we showed that our three-dimensional finite-element method [3,4] could be extended to describe high nonzero angular-momentum states [5,6], yielding a relative accuracy of 4 ppm in comparison with transition wavelengths obtained by recent experiments. Since these antiprotonic helium levels in practice could be described as bound with nonradiative fragmentation lifetimes of a few microseconds, we had to turn to doubly excited states of zero angular momentum in the normal helium atom [7] when trying to add the complex-scaling method [8] (CS) to our toolbox. Comparison with other similar studies then showed that our results were of comparable relative accuracy 10^{-5}.

The aim of our work is to be able to predict and/or analyze the analytic scattering theory structure behind reactive scattering phenomena, such as the HD+H or F+HD reactions, recently studied by Kendrick *et al.* [9] and Skodje *et al.* [10], respectively. However, we cannot do this safely before we make sure that our theoretical machinery works on problems where the interaction potentials are known and our results agree with experiment and accurate previous studies [11–18].

The normal helium atom represents such a benchmark system. In the present contribution we thus present results from nonzero angular momentum studies of doubly excited *P* and *D* levels of the normal helium. Improved results for our previously published doubly excited *S* levels of helium [7] are presented as a comparison of the extrapolation scheme and the numerical basis used here.

II. THEORETICAL APPROACH

The wave function of any three-body system with the total angular momentum L, projection m, and spatial parity τ can be represented by using eigenfunctions of the angular-momentum operator with respect to a body-fixed axis [19]. This amounts to an expansion in terms of Wigner *D* functions [20]:

$$\Psi^{L\tau}_{m}(\mathbf{R}) = \sum_{s}^{L} \frac{1}{\sqrt{2+2\delta_{s0}}} [D^{L}_{ms}(\alpha,\beta,\gamma) + \tau \times (-1)^{s} D^{L}_{m\,-s}(\alpha,\beta,\gamma)] \psi^{L\tau}_{s}(\mathbf{R}). \quad (1)$$

Here α, β, and γ are Euler angles, and $\mathbf{R}$ is a three-dimensional coordinate in the body-fixed frame, which is independent of α, β, γ. Index s varies as $s=0,1,\ldots,L$ for the positive parity $\tau=+1$ and as $s=1,\ldots,L$ for negative parity $\tau=-1$. In the following we shall omit the parity for the sake of simplicity.

Assuming an infinitely heavy nucleus, the body-fixed frame is conveniently specified by $\mathbf{R}=\{r_1,r_2,c\}$. Here r_i is the distance between the ith electron and the nucleus, $c=\cos(\vec{r}_1,\vec{r}_2)$. After substituting expansion (1) into the Schrödinger equation and using orthogonality relations for *D* functions [20], one can derive the following system of equations [5]:

$$-\left[\frac{1}{r_2}\frac{\partial^2}{\partial r_2^2}r_2-\frac{L(L+1)-2s^2}{r_2^2}+\frac{1}{r_1}\frac{\partial^2}{\partial r_1^2}r_1+\left(\frac{1}{r_1^2}+\frac{1}{r_2^2}\right)\right.$$
$$\left.\times\left(\frac{\partial}{\partial c}(1-c^2)\frac{\partial}{\partial c}-\frac{s^2}{1-c^2}\right)\right]\psi_s^L$$
$$+i\sqrt{1+\delta_{s0}}\,\frac{\lambda_+(L,s)}{r_2^2}\left(\sqrt{1-c^2}\,\frac{\partial}{\partial c}-(1+s)\frac{c}{\sqrt{1-c^2}}\right)$$
$$\times\psi_{s+1}^L+i\sqrt{1+\delta_{s1}}\,\frac{\lambda_-(L,s)}{r_2^2}\left(\sqrt{1-c^2}\,\frac{\partial}{\partial c}\right.$$
$$\left.-(1-s)\frac{c}{\sqrt{1-c^2}}\right)\psi_{s-1}^L=(E-V(r_1,r_2,c))\psi_s^L. \qquad (2)$$

Here $\lambda_\pm(L,s)=\sqrt{L(L+1)-s(s\pm1)}$, $\psi_{-1}^L\equiv0$, and we use the units with the electron mass $m_e=1$. A similar set of equations, obtained without the assumption of an infinitely heavy nucleus, is of the same complexity [5,21] but for comparison with other computational studies [11–18] we do not use here the equations with finite masses. The potential energy $V(r_1,r_2,c)$ is the sum of the Coulomb potentials:

$$V(r_1,r_2,c)=-\frac{2}{r_1}-\frac{2}{r_2}+\frac{1}{r_{12}}, \qquad (3)$$

where the interelectron distance is $r_{12}^2=r_1^2-2r_1r_2c+r_2^2$.

The components ψ_s^L must satisfy the boundary conditions so that

$$\psi_s^L(r_1,r_2,c)=(1-c^2)^{s/2}\tilde{\psi}_s^L(r_1,r_2,c), \qquad (4)$$

where $\tilde{\psi}_s^L(r_1,r_2,c)$ is a bounded function of its arguments.

Equation (2) is obviously nonsymmetric with respect to exchange $\vec{r}_1\leftrightarrow\vec{r}_2$. In fact, with the chosen body-fixed frame electron exchange symmetry cannot be implemented without loss of the block-three-diagonal structure of Eq. (2) [22]. While one can choose the body-fixed coordinates $\{\vec{r}_1+\vec{r}_2,\vec{r}_1-\vec{r}_2\}$ where the exchange symmetry manifests explicitly, we here use coordinates $\{\vec{r}_1,\vec{r}_2\}$ as they are more convenient in our numerical realization.

To calculate resonant states of the system in the CS method, we should replace the three-dimensional vectors $\vec{r}_i$ to the properly analytically continued complex ones. In fact, only the magnitudes r_i of the vectors have to be scaled [23]. For molecular systems, where the potential-energy surface is often known only as a set of closely spaced coordinate dependent numerical values that cannot be uniformly complex dilated, we need to use the exterior complex-scaling method of Simon [23] (ECS). We have experienced that the original sharp ECS introduces numerical instabilities that are compensated for by using the smooth exterior scaling method described by Helffer [24]. We thus define the transformation of r_i as follows [24]:

$$r_i\rightarrow\phi(r_i)=r_i+\lambda g(r_i), \qquad (5)$$

where $\lambda=\exp(i\theta)-1$, and θ is a dilation angle. Function $g(r)$ describes the complex path. We specify function $g(r)$ as

$$g(r)=\begin{cases}0, & r\leqslant R_0\\ (r-R_0)\{1-\exp[-\sigma(r-R_0)^2]\}, & r>R_0.\end{cases} \qquad (6)$$

The choice of the external radius R_0 and the curvature parameter σ is discussed in detail in Ref. [7]. The angular variable c is obviously not changed by the transformation.

In analogy with the uniform complex scaling [8], we define operator U_θ, which scales the wave function $\Psi(r_1,r_2,c)$, as

$$U_\theta\Psi(r_1,r_2,c)=p(r_1)p(r_2)\Psi(\phi(r_1),\phi(r_2),c). \qquad (7)$$

Here function $p(r_i)=\sqrt{|1+\lambda g'(r_i)|}$. As it was suggested in Ref. [25], it is convenient to deal with function $\Psi_\theta\equiv\Psi(\phi(r_1),\phi(r_2),c)$ without factor $p(r_1)p(r_2)$. The expression for the dilated Hamiltonian $H_\theta=U_\theta H U_\theta^{-1}$ acting on function Ψ_θ can be found in Ref. [7].

III. NUMERICAL REALIZATION

Numerically we have treated the present problem using the finite element method. One can find its description elsewhere [3,4,26], and details of our realization in Ref. [7]. The resonant energies $z=E-i\Gamma/2$ are obtained as eigenvalues of a functional $\langle\Psi_\theta|H_\theta|\Psi_\theta\rangle$. These energies are evaluated by solving a generalized eigenvalue problem:

$$\tilde{H}_\theta v=z\tilde{S}v, \qquad (8)$$

where

$$(\tilde{H}_\theta)_{im,jk}=\langle f_{im}|H_\theta|f_{jk}\rangle \quad\text{and}\quad (\tilde{S})_{im,jk}=\langle f_{im}|f_{jk}\rangle.$$

The basis functions f_{im} are expressed as products of one-dimensional functions. Such a representation of the basis functions simplifies an evaluation of the matrix elements in Eq. (8) and reduces the three-dimensional integrals of the kinetic energy to a product of one-dimensional ones. The one-dimensional basis functions were chosen to be associated Legendre polynomials $P_i^s(c)$ for the angular variable. Then the boundary conditions (4) are correctly taken into account. For the radial variables we have chosen a product of Legendre polynomials and an exponential function.

The generalized eigenvalue problem (8) was solved by the implicitly restarted arnoldi method [27]. For solving the set of linear equations appearing, we used the block LU factor-

TABLE I. Energies and widths (a.u.) of the *S* states in helium.

	Present		Extrapolated		References	
	E	Γ	E	Γ	E	Γ
$^1S^e$ (1)	-0.777869	0.004535	-0.777869	0.004543	-0.7778676	0.0045413 [a]
$^1S^e$ (2)	-0.621912	0.000213	-0.621915	0.000213	-0.6219273	0.0002156 [a]
$^1S^e$ (1)	-0.589897	1.374×10^{-3}	-0.589896	1.360×10^{-3}	-0.5898947	1.362×10^{-3} [a]
$^1S^e$ (2)	-0.548083	7.5×10^{-5}	-0.548084	7.5×10^{-5}	-0.5480855	7.48×10^{-5} [a]
$^3S^e$ (1)	-0.602578	6.8×10^{-6}	-0.602578	7.0×10^{-6}	-0.6025775	6.65×10^{-6} [a]
$^3S^e$ (2)	-0.559746	2.4×10^{-7}	-0.559747	2.8×10^{-7}	-0.5597466	2.6×10^{-7} [a]
$^1S^e$ (1)	-0.353541	3.015×10^{-3}	-0.353541	3.012×10^{-3}	-0.3535385	3.010×10^{-3} [a]
$^1S^e$ (2)	-0.317459	6.658×10^{-3}	-0.317458	6.664×10^{-3}	-0.3174578	6.660×10^{-3} [a]
$^1S^e$ (3)	-0.257364	2.1×10^{-5}	-0.257364	2.1×10^{-5}	-0.2573716	2.11×10^{-5} [a]

[a]Uniform complex scaling in perimetric coordinates, Ref. [12].

ization method. It is well known [8] that positions and widths of resonances are independent of the rotation angle θ. However, this is true only in exact calculations. When a numerical approximation is used, resonances become θ dependent. In this case, their positions E and widths Γ are defined by means of the complex variational principle [28]:

$$\left.\frac{dE}{d\theta}\right|_{\theta_r}=0 \quad \text{and} \quad \left.\frac{d\Gamma}{d\theta}\right|_{\theta_i}=0. \tag{9}$$

The two optimal angles θ_r and θ_i converge to one angle as the accuracy of the calculation increases.

IV. RESULTS AND DISCUSSION

In our calculations we have chosen maximum radii 50 a.u. for $n_1=n_2=2$ resonances and 70 a.u. for others. Five finite-element boxes were chosen for both r_1 and r_2 coordinates and one box for the c coordinate. The box boundaries are 1.24, 4.0, 6.6, and 16.0 a.u. The number of basis functions, p, was chosen to be 7 for the radial coordinates and 10 for the angular one. For the exterior scaling parameters, we use here the same values $R_0=4$ a.u. and $\sigma=0.25$ as in paper [7]. The matrix elements of the potential in Eq. (8) were calculated numerically using the 40-points Gauss-quadrature rule. This mesh yields sparse matrices of dimension 4530 with a total bandwidth of 2750 for each component.

These parameters coincide mainly with the parameters used in Ref. [7] for the calculation of the *S*-wave resonances. The only differences are increased maximum radius and increased number of integration points. These changes increase accuracy and explain a (very small) discrepancy between the results presented in Table I and in paper [7].

To check convergence, we also calculated extrapolated energy values using the formula [29]

$$E_{ext}=E_1+\frac{(E_1-E_0)(E_2-E_1)}{2E_1-E_0-E_2}, \tag{10}$$

where E_0, E_1, and E_2 are the energy eigenvalues obtained for $p=5$, 6, and 7. In the framework of the FEM, the asymptotic behavior for an approximate eigenvalue $E^{(p)}$ can, for rather small element volumes h and large polynomial degrees p, be written as

$$E^{(p)}=E^{exact}+Ch^{2p}, \tag{11}$$

where C is some constant [26]. One can then easily check that formula (10) gives the exact asymptotic energy: $E_{ext}=E^{exact}$. In this sense, using formula (10) is much better grounded for the FEM than for global basis function set methods [30]. While one should use formula (10) for finite (and not very big) values of p, it is shown [5] that already for moderate values of p, the asymptotic behavior (11) is accurately satisfied.

Using formula (10) in the frame work of the CS method poses some additional problems. First, the asymptotics (11) cannot be rigorously established for complex eigenvalues. Second, an additional complication arises from the dependence of energies on the rotation angle. As the rotated Hamiltonians are different for the different angles, we cannot use formula (10) for the optimal energy values obtained from condition (9). Instead, we should apply Eq. (10) separately for each angle, and then find the optimal [in the sense of Eq. (9)] value of the extrapolated energies.

This discussion is illustrated in Fig. 1, where we present the results for the $^3P^o(1)$ resonance. As expected, one can easily see that increasing of accuracy leads to the stabilization of the energy. The use of the extrapolation formula gives an even better result, stabilizing energy in a wider angle range. Based on this result and results presented in Tables I–III, we can draw the following conclusion about the possible use of the extrapolation formula (10) in the frame work of the CS Method. Because of the lack of the variational principle, it can hardly be used to improve the accuracy of the results. However, the extrapolation formula can serve as a useful tool to control the accuracy obtained. Moreover, Eq. (10) can facilitate an estimation of energies and optimal angles when the convergence is not yet reached.

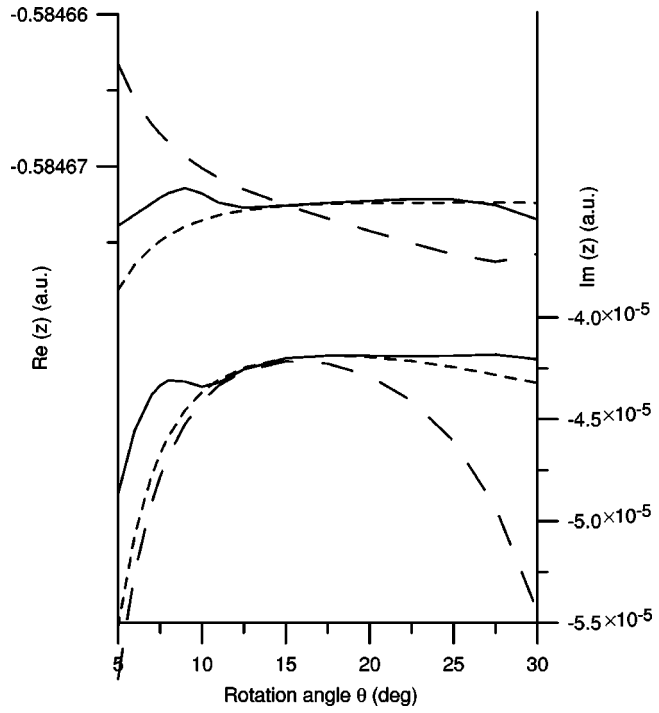

FIG. 1. The real (upper lines) and imaginary (lower lines) parts of the $^3P^o(1)$ resonance as a function of the rotation angle θ. The long-dashed lines correspond to E_1, the short-dashed lines correspond to E_2, and the solid lines correspond to the extrapolated energy values E_{ext}.

Our results for energy positions and widths are presented in Tables I—III. One can see that the difference between our values and other precise calculations [11–18] does not exceed 10^{-5} a.u., and is typically about few units of 10^{-6} a.u. Taking into account a rather modest size of the matrix, we can say that the combination of the total-angular-momentum representation, the finite-element method, and the smooth exterior complex scaling gives a reliable and accurate tool for a study of resonances in systems with nonzero angular momentum. One should also notice that the suggested method gives a comparable absolute accuracy for both real and imaginary parts or resonances in the sense that one here directly computes a complex eigenvalue $z=E-i\Gamma/2$. This means that for very narrow resonances, e.g., $^3S^e(2)$, $^1P^o(3)$, $^3D^e(1)$, the accuracy achieved in our calculations is of the same magnitude as the width. Hence, the widths of these resonances should only be estimated from above. We would like to note, however, that this comparability may not be a general case for every system. Indeed, we have performed computational studies of nonzero angular-momentum energies and predissociation widths based on the well-known model potential for the Ne-ICl van der Waals complex [21,31,32]. We have found that for that specific molecular system, the convergence of the widths is considerably faster than the convergence of the positions.

Concluding this paper, we would like to state that our smooth exterior complex scaling, full-angular-momentum, three-dimensional finite-element method is capable of yielding eigenenergies and corresponding widths for low angular

TABLE II. Energies and widths (a.u.) of the P states in helium.

	Present		Extrapolated		References	
	E	Γ	E	Γ	E	Γ
$^3P^e$	-0.710499		-0.710500		-0.7105002 [a]	
$^3P^o$	-0.760492	0.000298	-0.760491	0.000298	-0.7604924	0.0002989 [b]
$^1P^o$	-0.693128	0.001373	-0.693126	0.001370	-0.6931349	0.0013732 [c]
$^1P^e$	-0.580246		-0.580246		-0.58025 [d]	
$^3P^e$	-0.567813		-0.567813		-0.56781 [d]	
$^1P^o$ (1)	-0.597074	4.1×10^{-6}	-0.597073	4.0×10^{-6}	-0.5970738	3.85×10^{-6} [c]
$^1P^o$ (2)	-0.564084	3.04×10^{-4}	-0.564082	3.07×10^{-4}	-0.5640852	3.012×10^{-4} [c]
$^1P^o$ (3)	-0.547091	$4.\times10^{-8}$	-0.547091	$3.\times10^{-8}$	-0.5470927	1.05×10^{-8} [c]
$^3P^o$ (1)	-0.584672	8.38×10^{-5}	-0.584672	8.68×10^{-5}	-0.5846723	8.225×10^{-5} [b]
$^3P^o$ (2)	-0.579031	2.1×10^{-6}	-0.579031	2.1×10^{-6}	-0.5790310	1.89×10^{-6} [b]
$^3P^o$ (3)	-0.548844	$6.\times10^{-8}$	-0.548844	$8.\times10^{-8}$	-0.5488444	1.27×10^{-8} [b]
$^3P^e$ (1)	-0.336089	4.49×10^{-3}	-0.336089	4.490×10^{-3}	-0.3360879	4.489×10^{-3} [e]
$^3P^e$ (2)	-0.291157	7.4×10^{-5}	-0.291157	7.4×10^{-5}	-0.2911582	7.40×10^{-5} [e]
$^1P^o$ (1)	-0.335628	7.027×10^{-3}	-0.335628	7.027×10^{-3}	-0.3356259	7.023×10^{-3} [f]
$^1P^o$ (2)	-0.282826	1.463×10^{-3}	-0.282826	1.463×10^{-3}	-0.2828290	1.462×10^{-3} [f]
$^3P^o$ (1)	-0.350379	2.989×10^{-3}	-0.350374	2.991×10^{-3}	-0.3503777	2.987×10^{-3} [b]
$^3P^o$ (2)	-0.309380	1.118×10^{-3}	-0.309381	1.119×10^{-3}	-0.3093800	1.118×10^{-3} [b]

[a]Reference [13].
[b]Hylleraas wave functions with uniform complex scaling, Ref. [14].
[c]Uniform complex scaling in perimetric coordinates, Ref. [15].
[d]Uniform complex scaling, Ref. [11].
[e]Hylleraas wave functions with uniform complex scaling, Ref. [16].
[f]Hylleraas wave functions with uniform complex scaling, Ref. [17].

TABLE III. Energies and widths [a.u.] of the D states in helium.

	Present		Extrapolated		References	
	E	Γ	E	Γ	E	Γ
$^1D^e$ (3)	-0.701935	0.002359	-0.701935	0.002359	-0.7019457	0.0023622 [a]
$^1D^e$ (1)	-0.569219	5.55×10^{-4}	-0.569220	5.54×10^{-4}	-0.569221	5.55×10^{-4} [a]
$^1D^e$ (2)	-0.556429	2.1×10^{-5}	-0.556429	2.0×10^{-5}	-0.5564303	2.01×10^{-5} [a]
$^3D^e$ (1)	-0.583784	$2.\times10^{-8}$	-0.583784	$2.\times10^{-8}$	-0.5837843	2.86×10^{-8} [a]
$^3D^e$ (2)	-0.560686	$9.\times10^{-6}$	-0.560686	7.4×10^{-6}	-0.560687	7.5×10^{-6} [a]
$^1D^o$	-0.563800		-0.563800		-0.56380 [b]	
$^3D^o$	-0.559328		-0.559328		-0.55933 [b]	
$^1D^e$ (1)	-0.343174	5.157×10^{-3}	-0.343175	5.157×10^{-3}	-0.343173	5.155×10^{-3} [a]
$^1D^e$ (2)	-0.315533	4.293×10^{-3}	-0.315533	4.291×10^{-3}	-0.31553	4.305×10^{-3} [a]
$^1D^e$ (3)	-0.290083	1.263×10^{-3}	-0.290083	1.263×10^{-3}	-0.290092	1.261×10^{-3} [a]
$^3D^e$	-0.325331	7.25×10^{-4}	-0.325329	7.25×10^{-4}	-0.325331	7.25×10^{-4} [a]
$^1D^o$	-0.328233	3.21×10^{-4}	-0.328232	3.22×10^{-4}	-0.32823	3.21×10^{-4} [b]
$^3D^o$	-0.315575	2.087×10^{-3}	-0.315575	2.088×10^{-3}	-0.31558	2.09×10^{-3} [b]

[a]Hylleraas wave functions with uniform complex scaling, Ref. [18].
[b]Uniform complex scaling, Ref. [11].

momenta. As is seen from our previous antiprotonic helium studies, it is very likely that this may be extended to higher angular momenta. Therefore, the goal to have a precise computational tool to compute eigenenergies and widths for three-dimensional rotating systems, which can be represented by a single potential-energy surface, is in some sense reached. However, higher numerical accuracy can, in principle, be achieved by using the so-called adaptive ph scheme where the size of element h and the maximum degree of the basis polynomial p in the same element are chosen such that the residue of a given eigensolution of the Schrödinger problem in this element is smaller than a preset value [33].

The present method and its possible extensions remain to be tested on other atomic, molecular, and simple nuclear halo systems in order to identify boundaries of its applicability and to reveal properties of the systems associated with the nonzero angular momentum.

ACKNOWLEDGMENTS

S.L. acknowledges support by the National Science Foundation through a grant for the Institute for Theoretical Atomic and Molecular Physics at Harvard University and Smithsonian Astrophysical Observatory. S.L. also acknowledges support from the Royal Swedish Academy of Sciences and the Wenner Gren Foundations. A grant from the Swedish Research Council (former NFR) is also acknowledged.

[1] P.G. Hansen, A. S. Jensen, and B. Jonson, Annu. Rev. Nucl. Part. Sci. **43**, 591 (1995).
[2] R.S. Hayano *et al.*, Phys. Rev. A **55**, R1 (1997).
[3] A. Scrinzi and N. Elander, J. Chem. Phys. **98**, 3866 (1993).
[4] A. Scrinzi, Comput. Phys. Commun. **86**, 67 (1995).
[5] N. Elander and E. Yarevsky, Phys. Rev. A **56**, 1855 (1997); **57**, 2256 (1998).
[6] S. Andersson, N. Elander, and E. Yarevsky, J. Phys. B **31**, 625 (1998).
[7] N. Elander and E. Yarevsky, Phys. Rev. A **57**, 3119 (1998).
[8] M. Reed and B. Simon, *Methods of Modern Mathematical Physics* (Academic Press, New York, 1982), Vol. IV.
[9] B.K. Kendrick, R.T. Pack, R.B. Walker, and E.F. Hayes, J. Phys. Chem. **110**, 6673 (1999).
[10] R.T. Skodje, D. Skouteris, D.E. Manoloppoulos, S.-H. Lee, F. Dong, and K. Liu, J. Chem. Phys. **112**, 4536 (2000).
[11] E. Lindroth, Phys. Rev. A **49**, 4473 (1994).
[12] A. Bürgers, D. Wintgen, and J.-M. Rost, J. Phys. B **28**, 3163 (1995).
[13] A.K. Bhatia, Phys. Rev. A **2**, 1667 (1970).
[14] Y.K. Ho, Phys. Rev. A **48**, 3598 (1993).
[15] D. Wintgen and D. Delande, J. Phys. B **26**, L399 (1993).
[16] Y.K. Ho and A. Bhatia, Phys. Rev. A **47**, 2628 (1993).
[17] Y.K. Ho, Phys. Rev. A **44**, 4154 (1991).
[18] Y.K. Ho and A.K. Bhatia, Phys. Rev. A **44**, 2895 (1991).
[19] C.F. Curtis, J.O. Hirschfelder, and F.T. Adler, J. Chem. Phys. **18**, 1638 (1950).
[20] D. A. Varshalovich, A. M. Moskalev, and V. K. Khersonskii, *Quantum Theory of Angular Momentum* (World Scientific, Singapore, 1989).
[21] N. Elander, S. Levin, and E. Yarevsky, Phys. Rev. A **64**, 012505 (2001).
[22] A. Scrinzi, J. Phys. B **29**, 6055 (1996).
[23] B. Simon, Phys. Lett. **71A**, 211 (1979).
[24] B. Helffer, in *Resonances*, edited by E. Brändas and N. Elander, Lecture Notes in Physics Vol. 325 (Springer, Berlin, 1989).

[25] T.N. Rescigno, M. Baertschy, D. Byrum, and C.W. McCurdy, Phys. Rev. A **55**, 4253 (1997).
[26] K.W. Morton, Comput. Phys. Rep. **6**, 1 (1987).
[27] W.E. Arnoldi, Q. Appl. Math. **9**, 17 (1951).
[28] N. Moiseyev, P.R. Certain, and F. Weinhold, Mol. Phys. **36**, 1613 (1978).
[29] B. Schfiff, H. Lifson, C.L. Pekeris, and P. Rabinowitz, Phys. Rev. **140**, A1104 (1965).
[30] A. Kono and S. Hattori, Phys. Rev. A **31**, 1199 (1985).
[31] N. Elander, S. Levin, and E. Yarevsky, Nucl. Phys. A **684**, 678 (2001).
[32] N. Elander, S. Levin, and E. Yarevsky, Nucl. Phys. A **689**, 541 (2001).
[33] B. Szabò and I. Babuška, *Finite Element Analysis* (Wiley, New York, 1991).